Geothermics 127 (2025) 103266

Contents lists available at ScienceDirect

Geothermics

journal homepage: www.elsevier.com/locate/geothermics

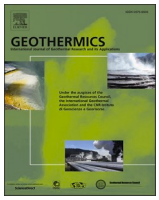

Impact of groundwater flow on thermal response tests in heterogeneous geological settings

Alberto Previati *, Giovanni Crosta

DISAT – Department of Earth and Environmental Sciences, University of Milano-Bicocca, Piazza della Scienza, 4, Milan 20126, Italy

ARTICLE INFO

Keywords:
Thermal response test
Groundwater flow
Advective heat transport
Moving infinite line source
Ground source heat pumps

ABSTRACT

This study investigates thermal response tests (TRTs) in heterogeneous geological settings to assess the impact of groundwater flow on TRT interpretation and borehole heat exchanger (BHE) performance. Traditional TRT analysis relies on the infinite line source (ILS) model, which assumes homogeneous ground and negligible groundwater flow. However, these assumptions are often lacking in natural environments, resulting in an overestimation of the thermal conductivity. The analysis of four distributed thermal response tests (DTRTs) in high groundwater flow regimes reveals apparent thermal conductivities up to 40 times higher than expected, highlighting the limitations of the ILS method in such settings. To address this issue, a comparison between the ILS model and the moving infinite line source (MILS) model, which accounts for advective heat transfer due to groundwater flow, was conducted. Model fitting and parameter optimization were performed on 84 temperature perturbation time series distributed along four BHEs used for TRT. The MILS model (global RMS = 0.25 °C) outperforms the ILS model (global RMS = 0.48 °C) in TRT data fitting and better reflects actual thermal conductivity values obtained from laboratory tests and literature. The MILS model also estimates groundwater flow velocities up to 3.0×10^{-5} m/s. Considering the estimated thermal conductivity and groundwater flow velocity, it was found that advective heat transfer contributes to 35–44 % of the total thermal exchange potential for all BHEs. A correction procedure for the apparent thermal conductivity derived from the ILS model, considering Darcy flow velocity, is presented using nomograms. This correction is crucial for accurate BHE design in areas with significant groundwater flow, ensuring a better understanding of BHE performance and its implications for shallow geothermal energy applications.

1. Introduction

Ground source heat pumps (GSHPs) represent a promising and increasingly adopted technology for heating and cooling buildings (Lund et al., 2022; Sanner, 2019). This growing popularity can be attributed to (at least) three key factors: I) GSHPs provide a heating solution with no direct GHGs emissions (Bayer et al., 2012; Self et al., 2013), II) they are deployable in most regions, making them broadly applicable (Curtis et al., 2005), and III) despite requiring electricity, their high efficiency ensures one of the lowest energy consumption levels among renewable heating technologies (Lo Russo et al., 2009; Saner et al., 2010; Self et al., 2013). This high efficiency is primarily attributed to the ground's high thermal diffusivity and thermal capacity, as well as its stable thermal regime, which is typically achieved at depths greater than 10 m. These characteristics make the ground a more consistent and reliable thermal energy source compared to other direct heating/cooling mediums, such as air or water. Thus, among all known configurations of GSHPs, vertical borehole heat exchangers (BHE) are mostly used to maximize the specific power output with respect to the installation costs (Aresti et al., 2018; Blum et al., 2011; Self et al., 2013).

In-situ thermal response tests (TRTs) are performed to design vertical GSHPs by deriving the compound ground/borehole thermal resistance of the BHE after recording the temperature evolution in time due to a constant heat power injection. This is typically achieved by keeping a constant temperature difference throughout a heat pump (HP) between the heat carrier fluid entering the BHE loop with respect to the fluid returning to the HP after the heat exchange. The TRT procedure and interpretation is widely used in practice (Galgaro et al., 2021; Sanner et al., 2008; Wilke et al., 2020) and described in many textbooks (Kavanaugh and Rafferty, 2014; Lamarche, 2023; Stauffer et al., 2013), and regulations (VDI 4640/5, 2020). To avoid interference of the initial fluid circulation and heat transfer through the borehole grout, previous

* Corresponding author.
E-mail address: alberto.previati@unimib.it (A. Previati).

https://doi.org/10.1016/j.geothermics.2025.103266
Received 11 November 2024; Received in revised form 20 December 2024; Accepted 23 January 2025
Available online 31 January 2025

studies indicated an optimal TRT duration of at least 20 to 60 h depending on site-specific characteristics (Gehlin, 2002; Spitler and Gehlin, 2015). The TRT interpretation method is based on the infinite line source (ILS) solution of the Fourier's law and was first presented by Carslaw and Jaeger (1959) and Ingersoll et al. (1954), and later developed for many GSHPs applications. This technique shows good accuracy in determining the effective ground thermal conductivity (λ) during a TRT upon the following assumptions: 1) the borehole is assumed to be an infinite vertical line of infinitesimal diameter (e.g., typically the vertical size is much larger than the horizontal; 2) the ground temperature and thermal properties are vertically homogeneous; 3) the effects of groundwater flow on heat transport are negligible. In practice, the last two assumptions are hard to satisfy in a natural environment. A common solution among GSHP designers is to consider vertically equivalent homogeneous thermal properties, following the principle of a purely radial heat flow oriented parallelly to the ground stratification (i.e., the homogeneous equivalent value corresponds to the thickness-weighted arithmetic mean of the single values of the strata). In recent developments, the vertical heterogeneity has been addressed by means of distributed thermal response test (DTRT) by recording the temperature evolution along the borehole length by means of thermistor strings or fiber optic temperature sensing (Wilke et al., 2020). Conversely, the last assumption is often neglected leading to misinterpretations of the ground thermal properties and GSHP performance when groundwater flow is present, and the TRT is interpreted by standard methods based on the ILS. The effect of groundwater flow on the heat propagation around BHEs and their resulting performance has been object of previous studies (Angelotti et al., 2014; Aresti et al., 2016; Chiasson et al., 2000; Previati and Crosta, 2024; Rivera et al., 2015; Wagner et al., 2013; Witte, 2013; Zhang et al., 2023; for a review, Zhao et al., 2022). Firstly, Diao et al. (2004) and Sutton et al. (2003) developed the analytical solution to estimate the temperature evolution around an infinite line source considering groundwater advection by means of the Green's function method, and Molina-Giraldo et al. (2011) developed an analogue solution for a finite line. The moving infinite line solution (MILS) approach has been recently adopted to interpret TRTs in advective dominated regimes (Albers et al., 2024; Angelotti et al., 2018; Antelmi et al., 2020; Simon et al., 2021), but a comprehensive procedure is still missing. For example, Wagner et al. (2013) proposed a correction to account for the hydraulic parameter contrast between the borehole grouting material and the surrounding ground. Simon et al. (2021) and Zhang et al. (2023) through combined actively heated and fiber optic cables (ETRT, according to Wilke et al., 2020) compared the MILS method with a graphic identification of the characteristic times for an improved estimation of the ground thermal conductivity and flow velocity. Although promising in several aspects, this technique remains so far poorly adopted in TRT analysis due to its high installation costs and the absence of a standardized method of interpretation, which this paper aims to contribute.

In this study, four traditional TRTs (Signorelli et al., 2007) were performed in the city of Turin (N Italy) and enhanced by incorporating 2.5 m-spaced thermistor strings inside auxiliary pipes in each borehole, obtaining four DTRTs with a total number of 84 temperature time-series. A comparison between all tests revealed that the standard interpretation of TRT and depth-distributed temperature perturbation time series from DTRT can lead to apparent thermal conductivity values up to 40 times the actual values. By comparing hydrogeological information from the test sites, this discrepancy was attributed to the advective heat transfer around the BHE induced by groundwater flow. This paper aims to quantify this effect. A comparison between the infinite line source (ILS) and the moving infinite line source (MILS) models, through data fitting and parameter optimization, highlights a significant overestimation of λ by the ILS model, particularly in regions with expected groundwater flow, where the MILS model is more suitable. Finally, a correction procedure of the apparent thermal conductivity (λ_{app}) obtained from the ILS method in advective-dominated regimes is proposed, emphasizing the role of Darcy flow velocity (v_d). The applicability and limitations of the ILS and MILS models in interpreting TRT data under high groundwater flow conditions are discussed.

2. Study site

Four in-situ thermal response tests (TRT), together with the DTRT tests performed simultaneously to the TRT tests, were analyzed in the scope of this work. The test sites are in the city of Turin (N Italy) and TRTs were conducted in 2022 along the pathway of the metro "Line 2″ for underground thermal characterization (Fig. 1a) as part of the installation of thermally active tunnel concrete walls (Barla et al., 2019).

Drillings for TRT (reaching 50 m of depth for TRTs 1, 2, 3 and 60 m for TRT 4) were performed by continuous rotation and core destruction. Thus, the lithostratigraphic vertical profile at each location (Fig. 1b) were reconstructed by matching the available nearby continuous-core drilling logs (Fig. 1a). For all the locations are available detailed borehole logs only up to 40 m of depth. Each TRT, except for TRT 4, crosses two main hydrogeological units (Festa et al., 2009): 1) a first shallow layer of Upper Pleistocene fluvio-glacial deposits pertaining to the 'Dora Riparia' basin (*Frassinere synthem*) made of pebbly heterometric gravels in a weakly-weathered sandy matrix, with no to moderate degree of cementation; 2) a deeper layer of marine deposits (*Argille Azzure or Marne di Sant'Agata Fossili fm.s*) made of silt, clayey silt and silty clay with thin levels of sandy silt, highly compacted with local lithification. The transition between the shallow and deeper units is marked by dashed lines in Fig. 1b, following the map of the shallow aquifer bottom provided by a regional study available on the regional geoportal (https://geoportale.igr.piemonte.it/). Note that for TRTs 1, 2 and 3 the proposed aquifer bottom agrees with the investigated lithostratigraphy, while for TRT 4 it is only suggested. The thickness of the saturated part of the shallow aquifer varies from a maximum of about 25 m at TRT4 to a minimum of 14 m at the center of the 'Dora Riparia' river valley axis (TRT2). The hydraulic gradient ranges from 1.9 to 6.3 ‰ showing the highest values close to the terraced topography of the 'Dora Riparia' river at TRT2.

3. Materials and methods

3.1. Test equipment

Four boreholes were drilled with a diameter of 152 mm to be used for vertical thermal response testing (TRT) and depth-distributed temperature recording (DTRT). The boreholes were equipped with single-U HDPE heat exchanger pipes having an external diameter of 40 mm and an internal diameter of 32 mm (Fig. 2), using shanks to maintain the distance between the pipes and to the borehole face. An auxiliary HDPE pipe of the same characteristics was installed in each bore, filled with water and equipped with a thermistor string with nodes every 2.5 m of depth to record the temperature evolution with an accuracy of 0.01 °C. TRTs 1, 2 and 3 (depth 50 m) had 20 nodes, while TRT 4 (depth 60 m) had 24 nodes in total. Finally, the borehole structure was cemented with thermal conductive grout having a nominal λ_{grout} of 2.3 W/mK.

The TRTs were performed using a portable heat pump machine and clean water as heat transfer fluid of the heat exchanger. During the tests, the temperature evolution of the fluid entering (T_{in}) and leaving (T_{out}) the heat exchanger, and at every node of the thermistor string was recorded with a sampling frequency of 15 min. The heating phase of each test lasted 48 h and the following recovery period was monitored for at least the same duration. A constant flow rate of 0.14 l/s and a 5 °C temperature difference between T_{in} and T_{out} were maintained throughout the test to ensure a total steady heat power (Q) delivery of approximately 3.45 kW to the ground. The specific power ($q = Q/L$) was retrieved considering the length of each BHE, the average measured flow rate and temperature difference recorded during each test, resulting in 70, 69, 69 and 58 W/m for TRT 1, 2, 3 and 4, respectively.

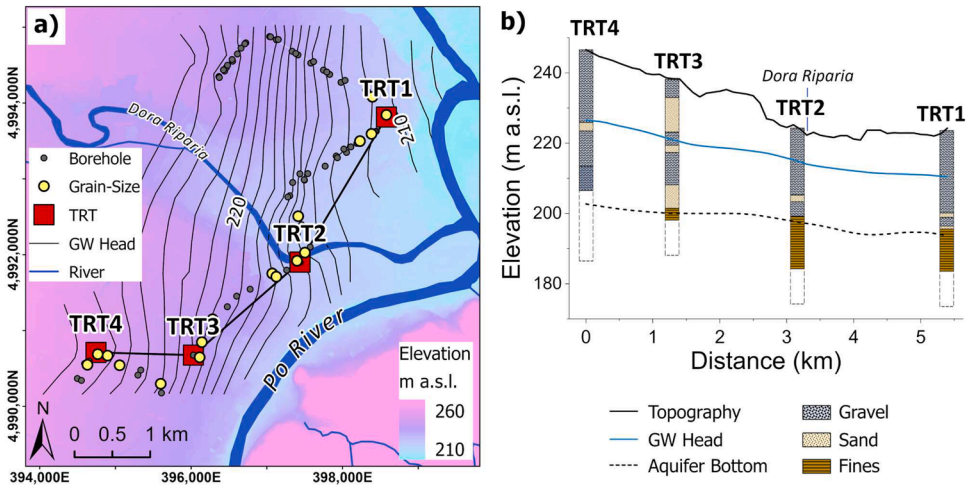

Fig. 1. (a) Map of the study site showing the location of the four thermal response tests (TRTs), the main hydrogeological features and the available borehole and grain-size information used in this work. (b) Simplified hydrogeological cross-section showing the lithostratigraphic characterization at each TRT site. DTRT at the same sites were acquired by 2.5 m-spaced thermistors inside auxiliary pipes.

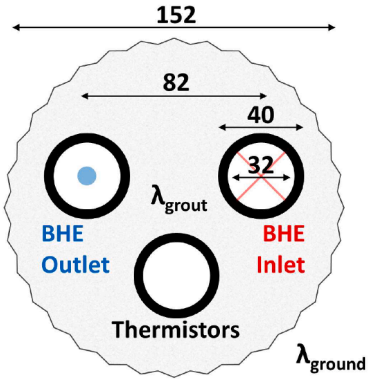

Fig. 2. Geometry and characteristics of the borehole heat exchanger (BHE) used for the TRTs. The bore is equipped with a thermistor string in the auxiliary pipe. All measurements are in mm.

Additionally, four disturbed and four undisturbed soil samples have been collected during borehole drilling to evaluate the thermal conductivity of the materials with the thermal needle method following the ASTM standard D5334–22. The disturbed samples were dried and reconstructed in a 8 cm-diameter cylindric sampler 10 cm high, at a bulk density of 2.0 kg/dm^3 after adding 18 % by weight of water. Finally, after thermal equilibrium of the samples at room temperature, the thermal conductivity was estimated using a 10 cm long needle. The test includes a heating and a recovery stage of 90 ss each, while the needle temperature is recorded every 2.5 ss. During the heating stage a constant heat power injection is provided by the instrument. According to the ILS analytical method, the effective thermal conductivity values (λ) are obtained comparing the heating and recovery stages. For each sample, the average between three measures of λ in different positions of the sample was adopted as a representative value.

Furthermore, grain-size analyses from soil samples collected along boreholes within a 500 m-radius from each TRT location were considered to reconstruct the lithostratigraphic profiles. Fig. 1a shows the location of the boreholes where grain-size analyses were collected.

3.2. Analytical methods

The thermal response test (TRT) results from the BHE inlet/outlet and from each node of the thermistor strings (DTRT) were analyzed through the methods described below and the vertical heterogeneity compared to the available lithostratigraphic and hydrogeological characteristics.

3.2.1. ILS method

The most widely adopted analytical model to interpret a TRT is founded on the infinite line source (ILS) theory (Carslaw and Jaeger, 1959; Ingersoll et al., 1954). The method approximates the radial temperature perturbation field around a heating line source upon the following assumptions:

- the vertical heating line source is of infinite length respect to the horizontal plane where the temperature field is examined;
- the temperature perturbation field is purely radial to the heat source axis, i.e. it can represent only a purely conductive heat transfer process;
- the initial temperature and the thermal resistance of the ground is homogeneous;
- the heat injection power is constant in time.

Although these assumptions are hardly fully satisfied in the geological environment, the ILS method is commonly adopted to interpret TRTs where the BHE is assumed to an infinite vertical line heat source of infinitesimal radius (Gehlin, 2002; Spitler and Gehlin, 2015).

The exponential integral solution provided by Carslaw and Jaeger (1959) can be approximated with Eq. (1), giving the temperature perturbation $\theta = T(t_i) - T(t_0)$ with respect to the initial temperature as a function of the radial distance (r) and time (t):

$$\theta_{\mathrm{ILS}}(r,t) = \frac{q}{4\pi\lambda}\cdot\left(\ln\frac{4\alpha t}{r^2} - \gamma\right) + q\cdot R_b \tag{1}$$

where q is the specific heat injection/extraction power (W/m), λ is the thermal conductivity of the ground (W/mK), $\alpha = \lambda/\rho c$ is the ground thermal diffusivity (ρc is the volumetric heat capacity of the ground), $\gamma = 0.5772\ldots$ the Euler's constant, and R_b the compound borehole thermal resistance.

The approximation of the integral solution for the infinite cylindrical problem given by Carslaw and Jaeger (1959) is valid for large values of the characteristic time ($t_c = r_b^2/\alpha$). It is widely recognized (after the work of Claesson and Eskilson, 1988) that the approximate solution produces negligible errors (<10 %) for $t > 5\,t_c$ which was also quantified numerically by Signorelli et al. (2007).

Moreover, according to Spitler and Gehlin (2015), the later stage (i.

e., typically after about 10 h) of a TRT have to be preferred to estimate the thermal conductivity of the ground. In fact, it was highlighted that the earliest times (i.e., in the order of 10–20 mins) of a TRT are affected by the circulation of warmed and not-yet-warmed fluids inside the BHE loop, while intermediate times (i.e., in the order of few hours) are affected by the heat transfer within the grout. Thus, only later times can assure the estimation of heat transfer properties inside the ground when the thermal front has penetrated beyond the borehole wall and the effects of the BHE can be neglected.

For these reasons, considering a broad range of possible ground thermal parameters λ and ρc between 1.0 to 3.0 W/mK and 1.5 to 3.0 MJ/m^{3}K (Dalla Santa et al., 2020; VDI 4640/2, 2001), respectively, the characteristic time (t_c) ranges approximately between 1 and 3 h and, consequently, the minimum required time for TRT analysis between 5 and 15 h. Thus, for each temperature time-series recorded during the TRTs, λ was estimated considering $t > 10$ h up to the end of the test (48 h).

Practically, from the experimental temperature-time evolution during the TRT, λ is determined taking the derivative of Eq. (1) with respect to the natural log of t. Therefore, ignoring all non-time-dependent terms, Eq. (1) yields to:

$$\lambda = \frac{q}{4\pi}\left(\frac{d\theta}{d(\ln(t))}\right)^{-1} \tag{2}$$

Therefore, the thermal conductivity can be also easily obtained graphically from the slope of the temperature plotted versus the logarithmic time.

Similarly, the ILS theory was applied to estimate the λ of the soil samples by means of the needle probe method in the laboratory. Eq. (2) was deployed comparing the slope of the temperature versus the logarithmic time for the heating (H) and recovery (C) stages. For the heating stages Eq. (2) was directly applied, while for the cooling stages the following transformation (Eq. (3)) is necessary to account for the duration of the heating phase before cooling:

$$\lambda_C = \frac{q}{4\pi}\left(\frac{d\theta}{d\left(\ln\left(\frac{t}{t-t_1}\right)\right)}\right)^{-1} \tag{3}$$

where t_1 is the total duration of the heating stage and q is the specific heating power applied constantly during heating. Representative values of λ will be provided in the results section considering the average between three measures in different positions of the sample.

3.2.2. MILS method

In natural aquifers, groundwater flow may have a significant impact on the heat transport (Angelotti et al., 2014; Aresti et al., 2016; Cai et al., 2020; Chiasson and O'Connell, 2011; Zhao et al., 2022). The importance of heat transport due to groundwater advection with respect to the conductive heat transfer is given by the thermal Peclet number:

$$Pe = \frac{v_e \cdot D}{\alpha} \tag{4}$$

where $v_e = v_d/n_e$ is the effective velocity obtained dividing the Darcy's velocity (v_d) by the effective porosity (n_e), and D represents the reference dimension, defined for this specific problem as the borehole diameter (2 x r_b). To quantify the thermal perturbation around a line source when groundwater flow is present, many studies (for a review, see Zhao et al., 2022) proposed analytical approaches to solve the partial differential equation of conduction-advection heat transport similarly to the conduction equation with a moving heat source through a fixed medium or with a fixed heat source in a moving medium. Diao et al. (2004) derived a solution (Eq. (5)) to this problem in transient conditions by means of the Green's function method:

$$\theta_{\mathrm{MILS}}(r,\varphi,t,v_t) = \frac{q}{4\pi\lambda}\cdot\exp\left(\frac{r\,v_t}{2\alpha}\cos\varphi\right)\cdot\int_0^{4\alpha t / r^2}\frac{1}{\eta}\cdot\exp\left(-\frac{1}{\eta}-\frac{r^2\,v_t^2\,\eta}{16\,\alpha^2}\right)d\eta + q\cdot R_b \tag{5}$$

where $v_t = v_d\,\rho c_w/\rho c$ is the effective heat transport velocity, φ is the polar angle, and $\eta = 4\alpha(t-t')/r^2$ is the integration parameter. The assumptions of this method are identical to those of the ILS method. An additional assumption is that the groundwater flow velocity is homogeneous and constant over time, oriented along the polar direction $\varphi = 0$. The assumption of a steady groundwater flow regime is justified by the short duration of the test (2 days) compared to the typical timescale of groundwater fluctuations in the region, which generally occur over weeks or months (e.g., seasonal or longer-term variations). Similarly, spatial homogeneity of the groundwater flow velocity can be assumed in the horizontal dimension, as the spatial scale of the perturbation caused by the test is smaller than the natural hydrogeological variability in the area. In the vertical dimension, however, characterizing the groundwater flow velocity distribution is the primary focus of this study.

Since the temperature on a circle around the heat source (e.g. at the borehole radius) is no longer constant, because of groundwater flow, the average temperature perturbation at a radial distance ($\bar{\theta}$) can be obtained by integrating Eq. (5) from 0 to π respect to the polar angle, giving:

$$\bar{\theta}_{\mathrm{MILS}}(r,t,v_t) = \frac{q}{2\pi\lambda}\cdot\mathrm{I}_0\left(\frac{r\,v_t}{2\,\alpha}\right)\cdot\int_0^{4\alpha t / r^2}\frac{1}{2\eta}\cdot\exp\left(-\frac{1}{\eta}-\frac{r^2\,v_t^2\,\eta}{16\,\alpha^2}\right)d\eta + q\cdot R_b \tag{6}$$

where I_0 is the modified Bessel function of the first kind of order zero used to express the integral function of the first exponential term of Eq. (5).

Simon et al. (2021) and Zhang et al. (2023) demonstrated that the minimum required time for evaluating heat transfer to the ground decreases from the theoretical characteristic time (t_c) defined for the ILS method as the flow velocity increases. This peculiarity ensures the minimum duration for TRT data fitting with the MILS method.

3.2.3. Surrogate advective g-function and thermal exchange potential

Another common approach to determine the spatial-temporal temperature perturbation around an infinite line source due to a constant heat rate is using nondimensional response functions also called *g-functions* (Eskilson, 1987; Kavanaugh and Rafferty, 2014; Spitler and Bernier, 2016). The *g-functions* have been firstly formulated as a complex integral equation or in the form of tabulated values by Carslaw and Jaeger (1959) and Ingersoll et al. (1954), and have been used to derive the temperature perturbation from the relationship:

$$\theta(r,t) = \frac{q}{\lambda}\cdot G(Fo) \tag{7}$$

where G is the *g-function* value for a given Fourier's number $Fo = \alpha t/r^2$.

Using the superposition principle, Eskilson (1987) firstly provided the ground response for different configurations of multiple boreholes and time-varying heat pulses, and many GSHP design softwares are based on this principle. The main limitation is that *g-functions* have been derived from the ILS theory and, thus, are valid only for purely conductive heat transport problems where the effect of groundwater advection is negligible.

The concept of *g-function* has been adopted by the authors (Previati and Crosta, 2024) for combined conduction-advection regimes by calculating numerically the mean radial temperature around a line source during constant heat injection and under variable Darcy velocity

values. A bundle of pseudo *g-functions* (G') was obtained by inverting Eq. (7) for different values of v_d and replacing $\theta(r,t)$ with the numerical results. The relationship $G'(Fo, v_d)$ was interpolated for a specific radius of 0.05 m by means of artificial neural networks (ANN) obtaining a surrogate model as displayed in Fig. 3.

A numerical regression of Fig. 3 was also obtained in the scope of this work from the results by Previati and Crosta (2024) and is given in the Supplementary Material.

Thus, the average temperature perturbation at a radial distance from the line heat source can be expressed using the numerically derived pseudo *g-function* $G'(Fo, v_d)$:

$$\overline{\theta}_{\mathrm{SRG}}(a,t,v_d) = \frac{q}{\lambda} G'(a \cdot Fo, v_d) \tag{8}$$

where a is a constant term used to account for a variable radius.

Alternatively, the values G' of the pseudo *g-function* were used by the authors (Previati and Crosta, 2024) to estimate the specific power extraction rates (P_{GSHP}) of the BHE following the ASHRAE method of Kavanaugh and Rafferty (2014) (a complete explanation of this method is given in the Supplementary Material, see Equation S.4):

$$P_{GSHP}\left(G'_{t1}, G'_{t2}, G'_{t3}, R_b, \Delta T, EFLH, COP, PLF, F_{sc}\right) \tag{9}$$

According to Kavanaugh and Rafferty (2014), the values of G' at three specific times: $t_1 = 4$ h, $t_2 = 30$ days and $t_3 = 10$ years were used to derive three corresponding ground thermal resistances R_{g1}, R_{g2} and R_{g3} (see Equation S.2 in the Supplementary Material) for short-, medium- and long-term heat pulses from the BHE to the ground.

The borehole thermal resistance (R_b) was calculated according to the characteristics following the method of Shonder and Beck (1999), considering the borehole radius (r_b), the BHE pipes radius (r_p), the number of pipes (n) and the thermal conductivity of the ground (λ_{grout}).

$$R_b = \frac{1}{2\pi\,\lambda_{grout}} \ln\left(\frac{r_b}{r_p\sqrt{n}}\right) \tag{10}$$

ΔT, *EFLH*, *COP*, *PLF* and F_{sc} depend on the GSHP configuration and refer, respectively, to the average temperature difference between the heat carrier fluid and the initial ground, the yearly equivalent full-load operating hours, the coefficient of performance of the system, the part load factor that accounts for the total daily operating hours, and the short-circuit factor depending on the BHE geometry.

Finally, the steps to determine the thermal exchange potential of GSHP with the method proposed by Previati and Crosta (2024) are summarized below (a complete explanation is given in the Supplementary Material):

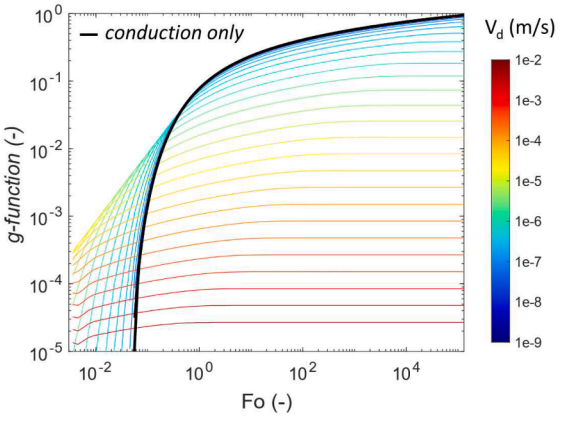

Fig. 3. Numerically derived pseudo g-functions (colored lines) expressed as a function of the Fourier number (Fo) for different Darcy velocities (v_d) compared to the static groundwater (conduction only) g-function solution (black line) (from Previati and Crosta, 2024).

1. from a set of synthetic numerical models, the pseudo *g-function* values (G') for GSHPs with groundwater flow were derived from the average temperature perturbation around the heating source using Equations (7) and (8);
2. pseudo *g-function* values (G') are calculated for three characteristic times $t_1 = 4$ h, $t_2 = 30$ days and $t_3 = 10$ years using the surrogate model by Previati and Crosta (2024) outlined in Fig. 3;
3. these G' values are implemented into the GSHP sizing method of Kavanaugh and Rafferty (2014) (ASHRAE), incorporating demonstrative system-specific parameters, to obtain P_{GSHP}.

3.2.4. Parameter estimation

The described analytical models were used to estimate the ground thermal parameter λ and the Darcy flow velocity v_d, assuming $r = r_b$. The following error functions were used to search for the optimal values of r, λ, α and v_D that best match the measured temperature evolution $\mathrm{T}(t)$ during the TRTs using the derivative-free method implemented in MATLAB:

$$\mathrm{E}_{\mathrm{ILS}}(r,\lambda,\alpha,R_b) = \sum_{i=0}^{n} \left[\mathrm{T}(t_i) - \theta_{\mathrm{ILS}}(r,t_i)\right]^2 \tag{11}$$

$$\mathrm{E}_{\mathrm{MILS}}(\lambda,\ v_d) = \sum_{i=0}^{n} \left[\mathrm{T}(t_i) - \overline{\theta}_{\mathrm{MILS}}(r,v_t,t_i)\right]^2 \tag{12}$$

Eq. (11) was used for ground parameter estimation (λ and α) from the average heat carrier fluid temperature (T_{avg}) time series. This equation was also used to estimate the borehole radius ($r = r_b$) and the compound borehole thermal resistance (R_b) and compare with their empirical estimations based on the geometry and characteristics of the boreholes. In the further analysis, r, R_b, and $c\rho = \lambda/\alpha$ will no longer be optimized and considered constant along the entire borehole length.

Eq. (12) was used for the estimation of local λ and v_d using the temperature time series measured at the thermistor string nodes (DTRTs). The results will be compared each other and against the available lithostratigraphic and hydrogeological knowledge of the sites.

4. Results

4.1. Thermal response test (TRT)

For each TRT, the average fluid temperature (T_{avg}) at each time step was calculated from the temperature of the fluid entering (T_{in}) and leaving (T_{out}) the heat exchanger. Fig. 4 displays the T_{avg} versus time for the four TRTs in comparison with the modeled temperature perturbation using the ILS method (Eq. (1)) after the optimization of λ, α and R_b by means of Eq. (11) with a fixed r of 0.075 m. For comparison, temperature perturbation time series from the DTRT are also shown. As suggested by the technical literature (Carslaw and Jaeger, 1959; Claesson and Eskilson, 1988; Signorelli et al., 2007; Spitler and Gehlin, 2015), to avoid disturbances due to the initial fluid circulation and heat transfer in the borehole grout, curve fitting and parameter optimization were performed only for $t > 10$ h.

The resulting optimal ground and borehole parameters for each TRT are displayed in Table 1 for $r = 0.075$ m.

Considering the materials described in Section 2, values of λ should range between 1.5 and 2.5 W/mK (Dalla Santa et al., 2020; VDI 4640/2, 2001) for the shallow unit and even lower for the deeper unit, suggesting a significant contribution of groundwater advection along the boreholes that may enhance the BHE-ground heat transfer processes leading to apparent higher values of TRT thermal conductivity.

Due to the indeterminacy of both λ and v_d using the MILS method (Angelotti et al., 2018), a range of possible values of v_d was assessed by optimizing v_d in Eq. (6) for a bundle of fixed values of λ. This was achieved by means of Eq. (12) adopting the estimated values of borehole thermal resistance in Table 1. Fig. 5 shows the optimal values of Darcy

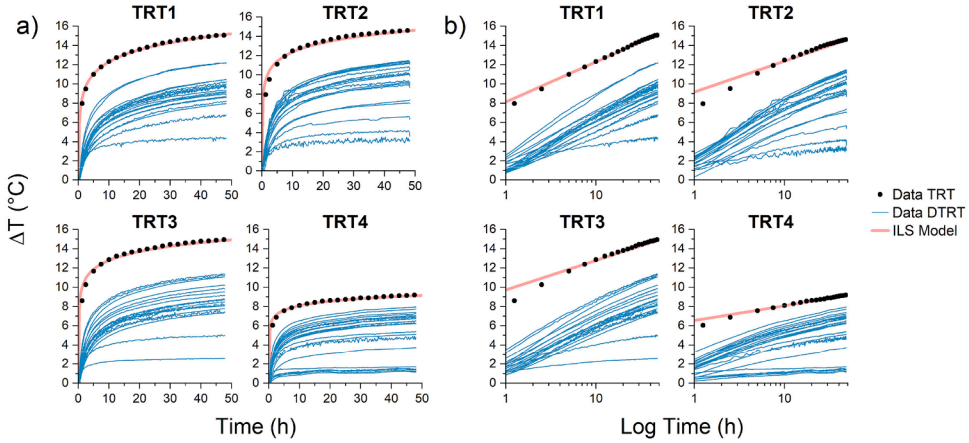

Fig. 4. TRT measured (empty dots) and calculated (red lines) temperature perturbation versus time (left) and logarithmic time (right), after the parameter estimation using the ILS method. Model fitting was performed for $t > 10$ h. The reader must note that the measured data are displayed every 2.5 h, while the real sampling frequency is 15 min. For comparison, temperature perturbation time series from the DTRT are also shown (blue lines).

Table 1
Optimal borehole and ground thermal parameters obtained with the ILS method. R_b is the borehole thermal resistance, λ is the ground thermal conductivity and $c\rho$ is the ground volumetric heat capacity. The optimal values of v_d using the MILS method are also shown for a range of λ between 1.5 and 2.5 W/mK.

	TRT1	TRT2	TRT3	TRT4
R_b (mK/W)	0.10	0.12	0.13	0.10
$c\rho$ (J/m^{3}K)	2.649×10^6	2.50×10^6	2.36×10^6	2.52×10^6
λ_{ILS} (W/mK)	3.08	3.94	4.12	6.91
v_d(m/s)	$2.78 - 4.76 \times 10^{-6}$	$4.86 - 6.01 \times 10^{-6}$	$5.07 - 6.28 \times 10^{-6}$	$9.20 - 10.0 \times 10^{-6}$

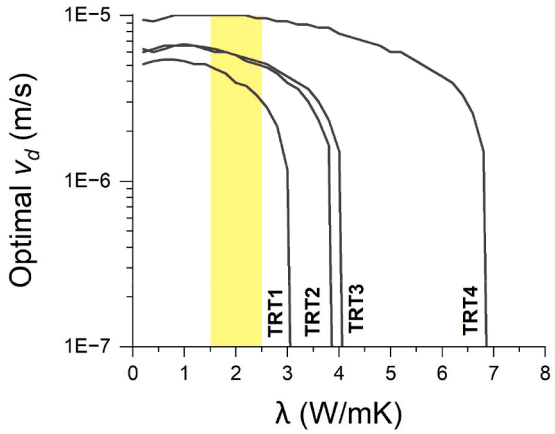

Fig. 5. Optimal values of Darcy flow velocity (v_d) obtained for a bundle of thermal conductivity values (λ) for each TRT. The yellow area shows the most likely interval for λ according to the geological materials described in Section 2.

flow velocity (v_d) obtained for a bundle of thermal conductivity values (λ) for each TRT, highlighting the different contribution of advection in each TRT. It is important to note that as λ increases, the optimal v_d approaches a vertical asymptote corresponding precisely to the λ value estimated using the ILS method. Conversely, as λ decreases, the optimal v_d reaches a maximum value. Resulting intervals of v_d for the range of λ between 1.5 and 2.5 W/mK are given in Table 1.

4.2. Distributed thermal response test (DTRT)

The vertical variability of the thermal exchange properties between the ground and the BHE, along with the contribution of conductive and advective processes, was investigated by analyzing 84 temperature time series (Fig. 6) recorded along the BHE every 2.5 m from four thermistor strings installed inside each TRT borehole. This technique is also known as distribute thermal response testing (DTRT). The normalized temperature ($\theta_q = \theta/q$) time-depth heat maps show a strong vertical heterogeneity in the borehole-ground heat transfer processes after the constant heat power injection deployed by the TRTs. It is clearly visible the presence of small layers with a significant contribution of groundwater advection whose characterization is object of this work. From Fig. 6, especially in the cooling stage, it is also visible the vertical heat transfer between the layers which is not addressed in this work.

Temperature time series from DTRTs were analyzed by means of the ILS and MILS methods to retrieve the optimal conductive and advective BHE-ground heat transfer parameters. The results are plotted against depth in comparison with the lithostratigraphic profiles and the available grain-size data in Fig. 7.

As outlined by the configuration of the BHE (Fig. 2) and the recorded temperature differences during the TRTs (Fig. 4), the thermal resistance (R_b) for the DTRT temperature time series is lower than the one calculated for the standard TRT (shown in Table 1). This difference can be attributed to the outermost positioning of the auxiliary pipes where the thermistor strings are located. To estimate the equivalent R_b at the measurement position of the DTRTs, the ILS method was applied to all temperature time-series for each DTRT using Eq. (11). A single value of R_b was assumed for each location (since the geometric configuration remains consistent along the borehole), while the thermal conductivity (λ) was allowed to vary at each depth level. The resulting values of R_b were 0.019, 0.035, 0.027 and 0.010 mK/W for DTRT 1, 2, 3 and 4, respectively. These values are notably lower than those calculated using the temperature difference between the inlet and outlet pipes and will therefore be neglected in the subsequent processing of the DTRT series. This approach is further justified by the fact that fitting was performed for $t > 10$ h, ensuring that only heat transfer processes in the ground are considered.

Additionally, introducing another parameter into the optimization process of the MILS method would increase the degrees of freedom, potentially complicating the estimation of v_d, as addressed later. However, it is important to acknowledge that neglecting R_b, while having a minimal effect on the DTRT, could result in a slight underestimation of

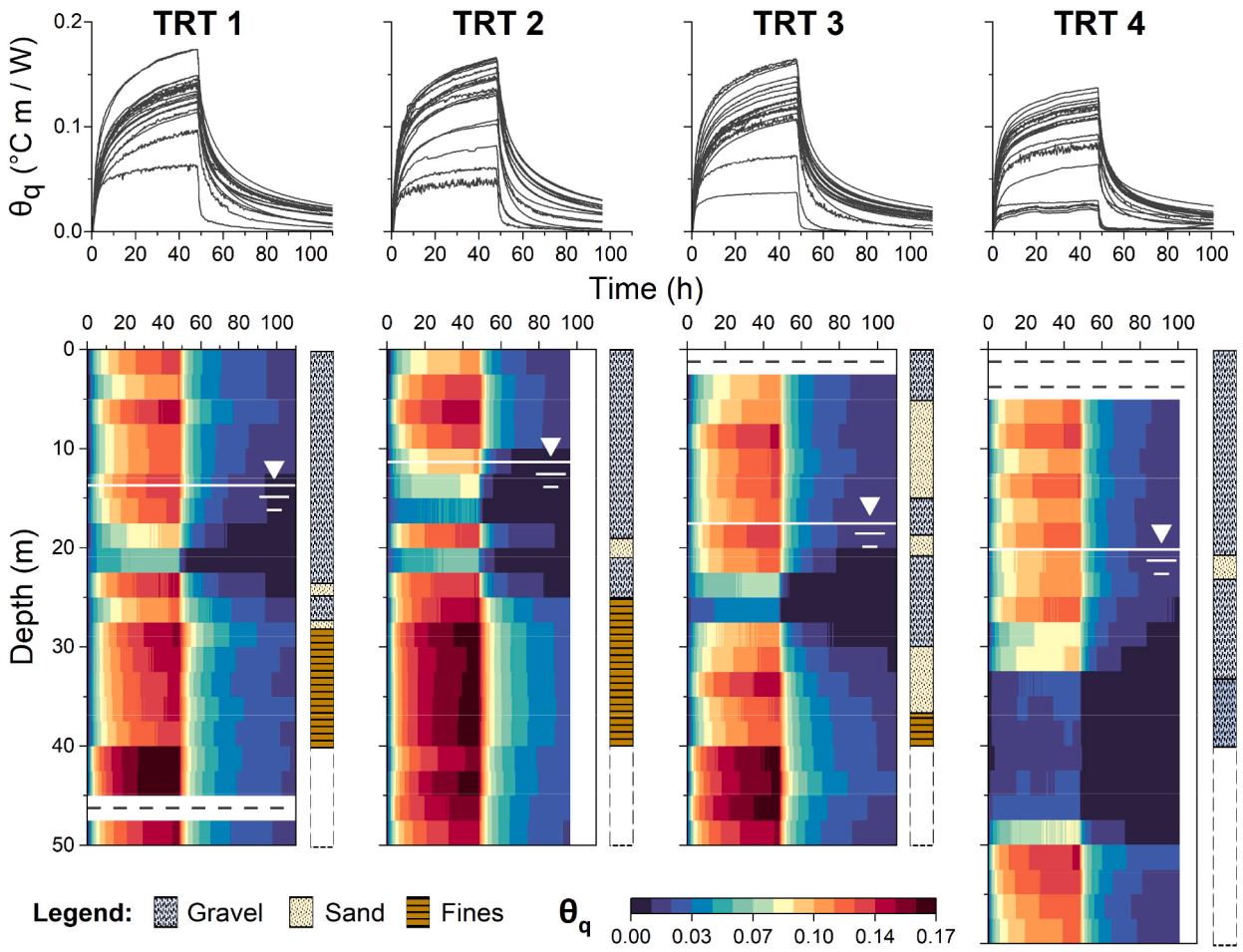

Fig. 6. Depth-distributed TRT temperature perturbation data from the thermistor strings at each borehole (from TRT1 to TRT4) plotted as time-series (upper plots) and as time-depth heat maps (lower plots). θ_q = temperature perturbation normalized by the average specific heating power (q) of each test. The white lines in the lower plots show the depth of groundwater, while the dashed horizontal lines show missing data due to interference with the heat flow at the ground-surface interface or recording problems. The lithostratigraphic profile for each borehole is plotted to the right of each heatmap.

v_d or λ values, as demonstrated by Eq. (6).

Fig. 7a shows the depth-distributed values of λ obtained by the ILS method (Eq. (1)) on each temperature time series (DTRT) in comparison with the mean value of λ obtained by the ILS method on the average fluid temperature (T_{avg}) from TRT as shown in Table 1, and the optimal values of λ obtained by the MILS method after optimization of the groundwater velocity (v_d) for each depth level (DTRT). For the MILS method, two parameters optimization attempts were made: one without any constraint on all parameters (MILS in Fig. 7) and another constraining the λ between 1.5 and 2.5 W/mK ($MILS_{CO}$ in Fig. 7). In the same plot, the values of laboratory-estimated λ for specific soil samples by means of the needle probe method are also shown. These lasts, generally exhibit lower values than in-situ estimates, probably due to the lower time and spatial scales of investigation achieved with the laboratory method and the absence of moving groundwater.

The high (up to 10 - 40 W/mK) apparent values of λ displayed in Fig. 7a by the ILS method are compensated by the combination of lower optimal values of λ and values of v_d using the MILS solution. These high values of groundwater flow are not only necessary to explain the high BHE-ground heat transfer capacity shown by some depth levels but are also confirmed by the lithological profiles and the available grain size information.

Fig. 7b shows the optimal Darcy groundwater flow velocity (v_d) for each depth level attained by means of the MILS method constraining λ between 1.5 and 2.5 W/mK as a realistic range derived from the laboratory needle probe analysis. The abundance of fines (i.e., $d < 0.075$ mm) by weight derived from the available grain-size analyses is shown for comparison. The grey dashed area shows the likelihood range of v_d obtained by optimizing v_d from Eq. (12) for the boundary values of λ (= 1.5 and 2.5 W/mK, respectively). This analysis demonstrates that for high flow velocity values, where the advective contribution outweighs the conductive one (i.e., for Pe > 2), the range of possible v_d values narrows significantly, indicating that this parameter is essential for interpreting the local thermal response. Conversely, where the advective contribution is negligible or absent, the range of possible v_d values broadens, as its role in determining temperature development is null. This leads to the indeterminacy of v_d in conduction-dominated regimes (e.g., for Pe < 2 or v_d below 2.5×10^{-6} m/s), where estimating v_d using the MILS model on TRT data becomes unfeasible.

In practical terms, v_d is a key parameter for predicting the ground thermal response in advective-dominated regimes, while in conductive regimes, its indeterminacy increases due to its limited influence on local thermal processes agreeing to the conclusions by Angelotti et al. (2018).

Vertically-equivalent values of v_d were retrieved for each DTRT by computing the depth-weighted average of depth distributed values of v_d and compared to the values of v_d obtained applying the MILS method on the average (T_{avg}) BHE temperature (Table 2), demonstrating good agreement and supporting the acceptability and comparison between

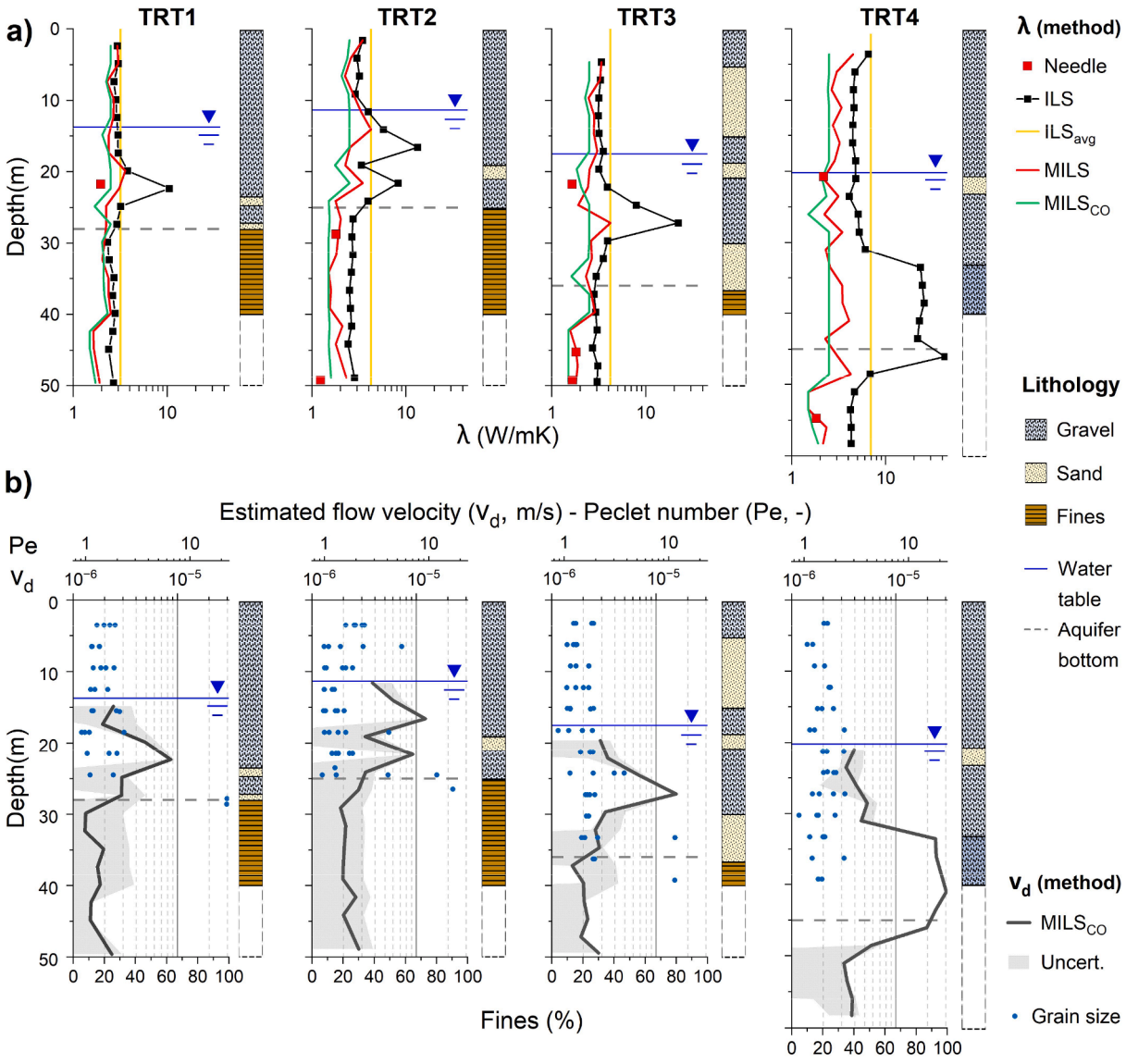

Fig. 7. (a) Estimated values of thermal conductivity (λ): Needle – in the laboratory by the needle probe method (ASTM standard D5334–22), ILS – infinite line source method (Eq. (1)) on depth-distributed temperature time series (DTRT), ILS_{avg} – infinite line source method on the average fluid temperature (TRT), MILS and $MILS_{CO}$ – moving infinite line source method (Eq. (6)) after the optimization of v_d and λ at each depth for each borehole, without constraints (MILS) and constraining ($MILS_{CO}$) the λ between 1.5 and 2.5 W/mK, respectively (DTRT). (b) Estimated values of Darcy groundwater flow velocity (v_D) using the MILS method: black line = optimal value, grey dashed area = uncertainty range obtained for $1.5 < \lambda < 2.5$ W/mK; in comparison with the available grain size data from borehole sampling (expressed as percentage of fines, i.e., $d < 0.075$ mm, by weight in each sample). The Peclet number (Pe) is displayed considering $\lambda = 2$ W/mK, $\alpha = 8 \times 10^{-7}$ m^2/s, $D = 0.152$ m, $n = 0.25$. The groundwater depth as of August 2022 and the estimated bottom of the shallow layer of highly permeable deposits are displayed as horizontal lines for each borehole.

Table 2
Vertically-equivalent Darcy flow velocity (v_d) obtained with the MILS method on the average BHE fluid temperature (T_{avg}) and by the depth-weighted average of depth distributed values of v_d (from DTRT). The resulting borehole-equivalent horizontal hydraulic conductivity (K) was derived considering the local hydraulic gradient (i).

	TRT1		TRT2		TRT3		TRT4		
i (‰)	2.8		6.3		6.2		1.9		
	T_{avg}	DTRT	T_{avg}	DTRT	T_{avg}	DTRT	T_{avg}	DTRT	
v_d (m/s)	2.8 – 4.8	1.9	4.8 – 6.0	3.0	5.0 – 6.3	2.6	9.1 – 10	8.3	x 10^{-6}
K (m/s)	1.0 – 1.7	0.69	0.8 – 0.9	0.48	0.8 – 1.0	0.43	4.8 – 5.2	4.4	x 10^{-3}

the classical interpretation of TRT and the DTRT method with the MILS approach. The resulting equivalent horizontal hydraulic conductivity ($K = v_d/i$) was obtained for each TRT from the observed hydraulic gradient (i) showing agreement between the two methods and, in general, with typical values of K expected for the geological materials described.

4.3. Thermal exchange potential

Finally, by applying the surrogate model approach by Previati and Crosta (2024) (see the Supplementary Material for a detailed explanation), the GSHP thermal exchange potential (P_{GSHP}) was obtained for

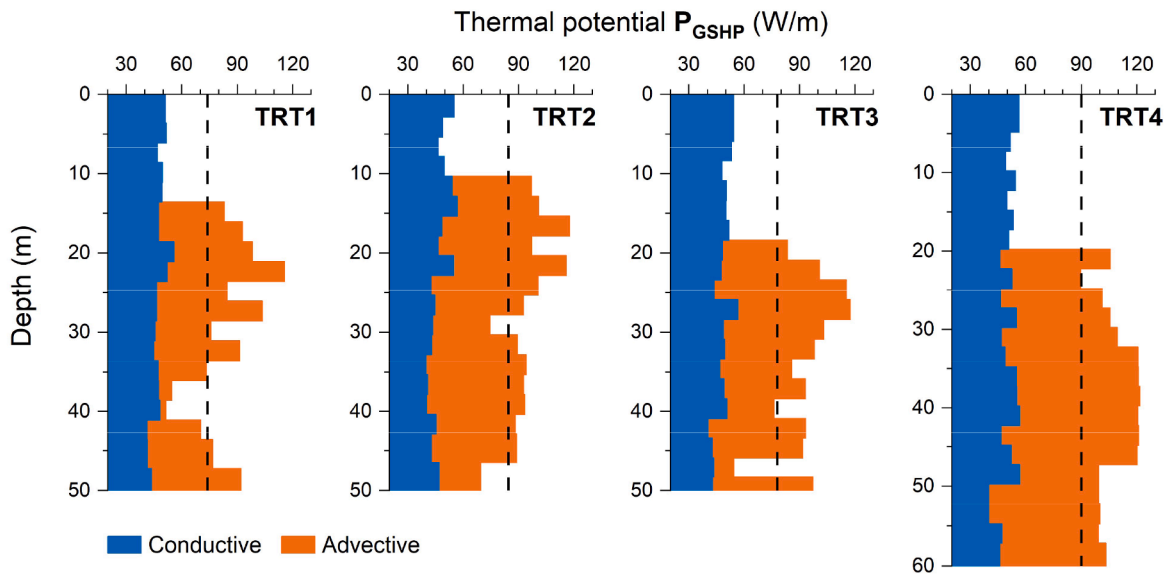

Fig. 8. Depth-distributed values of GSHP thermal exchange potential (P_{GSHP}) in W/m obtained by the model by Previati and Crosta (2024) from the optimized parameters λ and v_d of the MILS model. The blue area represents only the conductive contribution (obtained setting $\boldsymbol{v_D} = 0$) and the orange area represents the additional advective contribution obtained using the estimated values of λ and v_d. The dashed vertical lines the depth-averaged P_{GSHP} obtained by the model considering conduction and advection.

each depth level considering the values of λ and v_d obtained by parameter optimization of the MILS model (Eq. (6)). Fig. 8 shows, for each TRT, and for each depth level, the values of P_{GSHP} obtained by the surrogate approach considering only conduction (i.e., using the MILS-estimated values of λ from Fig. 7a and setting $v_d = 0$) and both conduction and advection (i.e., using the MILS-estimated values of λ from Fig. 7a and v_d from Fig. 7b).

The depth-averaged values of P_{GSHP} for BHE in TRT1, 2, 3 and 4 are 47.4, 46.7, 48.7, 50.4, and 73.9, 84.4, 77.9, 90.2 W/m considering only conduction or conduction and advection, respectively. Thus, the estimated contribution of groundwater advection on the specific power extraction rates of the BHEs stands at the 35, 44, 37 and 44 % of the total, respectively for TRT1, 2, 3 and 4.

5. Discussion

Distributed thermal response tests (DTRT) indicate high heat exchange rates between the BHE and the ground where the presence of high groundwater flow is suggested by the available hydrogeological information. This study aligns with previous findings dealing with the quantification of the groundwater flow contribution during a TRT (Angelotti et al., 2018; Antelmi et al., 2020; Chiasson and O'Connell, 2011; Zhang et al., 2023) for a set of very high (up to 3.0 × 10^{-5} m/s), yet unexplored, groundwater velocity values.

The combined advective-conductive MILS heat transport model was used to retrieve their respective contributions on the BHE-ground heat exchange, and to estimate the magnitude of groundwater flow along the BHEs. With a global RMS between all measured and simulated DTRT temperature perturbations of 0.25 °C, the MILS solution generally outperforms the purely conductive ILS solution (with a global RMS of 0.48 °C).

Considering the average hydraulic gradient of 2 to 6 ‰, it was observed that a hydraulic conductivity between 4.3 × 10^{-4} and 4.4 × 10^{-3} m/s is required to achieve the estimated flow velocities corresponding to the observed heat exchange rates. These values are typical of the described materials where vertical heterogeneities, such as preferential flow channels, can locally increase the groundwater flow significantly. These high velocities are able to capture a great portion of the total heat exchanged by the vertical BHE and their thermo-hydrogeological investigation is essential for shallow geothermal applications.

A possible limitation of the presented DTRT analysis lays in the assumption of a vertically homogeneous heating load (Q) distribution along the BHE. In practice, this is related to the actual temperature difference between the heat carrier fluid and the surrounding ground for every depth level of the BHE, leading to possible non-homogeneous distribution of the applied specific heat extraction rate (q). The homogeneity assumption may be considered acceptable for TRT1, 2 and 3, since they exhibit a quite constant initial temperature-depth distribution as shown in Fig. S1 (in the Supplementary Material). Conversely, TRT4 displays a strong vertical heterogeneity of the initial temperature-depth distribution possibly due to the presence of two geothermal injection wells (groundwater heat pumps, GWHP) located 90 m upgradient (described in the work by Lo Russo et al., 2011). Thus, higher uncertainty must be expected on the assessment of the heat transfer along TRT4 since the higher heat exchange values estimated between 32.5 and 50.0 m of depth (Fig. 6b) might be overestimated due to the higher initial temperature values shown in Fig. S1 and confirmed by the geothermal reinjection wells filter screen interval.

This limitation has been resolved by the novel enhanced thermal response test (ETRT) technique (Dalla Santa et al., 2022; Wilke et al., 2020; Zhang et al., 2023) where a combined heating-fiber optic cable is used to control the applied heating load, or by using multiple fiber optic cables inside the BHEs (Acuña et al., 2011; Acuña and Palm, 2013). In the work of Albers et al. (2024), the specific heating power q was retrieved for each depth level by coupling the ETRT techniques with fiber optic temperature sensing, while Acuña et al. (2011) resolved q from a local energy balance across coaxial BHEs from multiple fiber optic temperature sensing. This study configuration, which excludes the estimation of local heat fluxes across the BHE and assumes a homogeneous specific heating power load (q), recognizes the potential for parameter misestimations arising from inaccuracies in local q values.

5.1. Nomograms for the interpretation of TRTs considering the effect of groundwater flow

Nevertheless, the present work provides valuable insights into when it is appropriate considering groundwater flow and how it can be

effectively incorporated into TRT analysis. However, in common practice, the MILS method (Eq. (6)) is not frequently adopted due to the greater complexity of the equation with respect to the ILS method (Eq. (1) and (2)), which is widely used and mentioned by the TRT guidelines but inappropriate in advective hydrogeological regimes as demonstrated by this study and in the literature. Therefore, a method was presented to derive the actual thermal conductivity (λ) from the apparent thermal conductivity (λ_{app}), which arises from the improper application of the ILS method to groundwater advection-dominated TRT data.

The relationship between λ and λ_{app} was investigated comparing the ILS and MILS solutions to a range of synthetic thermal perturbation time series generated with the MILS method and varying the groundwater flow velocity (v_d), obtaining the theoretical nomograms presented in Fig. 9.

Fig. 9 shows the ratio λ_{app}/λ versus (a) the groundwater flow velocity (v_d), and (b) the actual thermal conductivity (λ), for different values of λ and v_d, respectively. Black dots represent the values from DTRT and TRT analyses presented in this study where the λ_{app} was obtained applying the ILS method to the measured temperature perturbation time series, while λ was obtained with the MILS method after the optimization of both λ and v_d as described in the previous section.

In practice, the nomograms shown in Fig. 9 can be used by varying the combination of λ and v_d within a range of reasonable values to obtain λ from λ_{app} and v_d, or to estimate $v_d$from λ and λ_{app}. This approach can be useful, for example, assuming that the hydrogeological regime in a study area may vary over time due to natural or anthropogenic forcing, to refine the estimates of the thermal exchange potential (P_{GSHP}) resulting from the TRT.

These plots also display two main limitations of the proposed approach. First, several combinations of λ and v_d may lead to very similar temperature perturbations over time using the MILS equation introducing uncertainty in the optimization process if none of the two parameters is known in advance (as discussed by Angelotti et al., 2018) which may be reduced introducing plausible boundaries for λ to narrow the possible space of solutions for v_d. For practical applications, this work demonstrated that the non-uniqueness of the λ and v_d estimations from TRT data is problematic only for purely conductive and conductive-advective transitional regimes (i.e., for Pe < 2), where the effects of groundwater flow on heat transport is negligible and, therefore, the ILS solution becomes reliable. For advective dominated regimes (i.e., for Pe > 2), it was demonstrated that v_d is essential for TRT data fitting and, therefore, predicting the ground thermal response. Moreover, in such cases, the range of possible v_d narrows as the ratio of advection to conduction contributions increases (i.e., as the Peclet number rises), thereby enhancing the reliability of the MILS solution.

The second limitation was highlighted by the comparison of the proposed theoretical nomograms with real interpreted data from TRTs (black dots in Fig. 9a) revealing significant deviations. In particular, in the upper-right corner, very high values of λ_{app}/λ can be simulated only adopting flow velocities higher than the theoretical expectations probably to compensate the thermal resistance of the borehole grout which is not included in the nomograms. Minor discrepancies may also be due to the vertical heat transfer which is neglected by this model.

6. Conclusions

This study underscores the significant influence of groundwater flow on thermal response tests (TRTs), challenging traditional approaches that assume ground homogeneity and ignore groundwater effects. The application of both the infinite line source (ILS) and moving infinite line source (MILS) models to TRT data revealed the overestimation of the thermal conductivity (λ) by the ILS method in advective dominated regimes. In particular, for values of Darcy velocity (v_d) greater than 5×10^{-6} m/s, the traditional ILS approach leads to apparent values of λ up to 40 times larger. The MILS approach, which accounts for advective heat transfer, provides a more accurate interpretation of the heat transfer in the ground, estimating both λ and v_d.

The analyzed depth-distributed TRTs show strong vertical heterogeneity in the heat transfer, with few layers displaying significant groundwater advection with local values of v_d up to 3×10^{-5} m/s. Their contribution on the total heat exchanged by the BHE was quantified thanks to a surrogate model for geothermal potential assessment developed by the authors. It was discussed that the advective contribution to the specific power extraction rates of the BHEs (i.e., the shallow geothermal potential) accounts for 35–44 % of the total heat extraction capacity. Moreover, it has been demonstrated that the non-uniqueness of v_d values when fitting TRT data diminishes as the advection to conduction ratio increases, making the estimation of v_d increasingly reliable as its value grows. These findings emphasize the need to account for both conduction and advection when estimating geothermal potential of GSHPs.

Finally, a correction procedure is proposed to adjust the apparent thermal conductivity derived from improperly interpreted TRT data by the ILS method in advective regimes, incorporating the effect of groundwater flow velocity through a nomogram approach. This research provides an improved framework for interpreting TRT data for

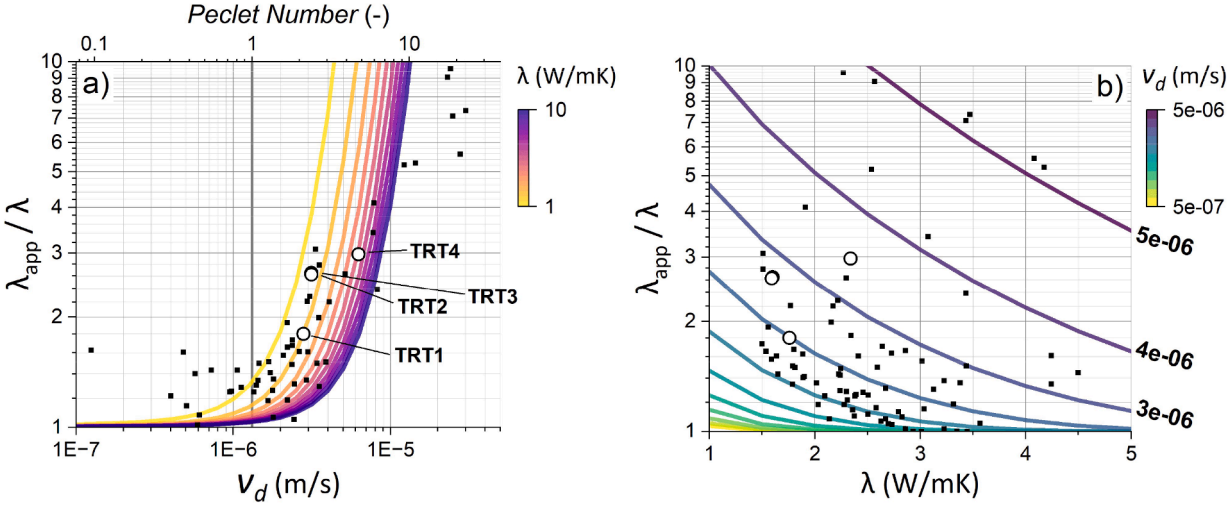

Fig. 9. Nomograms of the ratio λ_{app}/λ versus (a) the groundwater flow velocity (v_d), and (b) the actual thermal conductivity (λ), for different values of λ and v_d, respectively. The apparent thermal conductivity (λ_{app}) was obtained with the ILS method for different values of flow velocity. The dots in both plots (black = from DTRT data, empty circles = from T_{avg} TRT data) show the λ_{app}/λ values obtained in this study after the estimation of v_d and λ with the MILS method.

various hydrogeological regimes, considering groundwater flow, leading to more reliable GSHP designs and geothermal potential assessments, promoting the sustainable use of shallow geothermal energy.

CRediT authorship contribution statement

Alberto Previati: Writing – original draft, Visualization, Software, Methodology, Formal analysis, Data curation, Conceptualization. **Giovanni Crosta:** Writing – review & editing, Validation, Supervision, Funding acquisition.

Declaration of competing interest

The authors declare that they have no known competing financial interests or personal relationships that could have appeared to influence the work reported in this paper.

Acknowledgments

The authors gratefully thank *InfraTO srl* for providing the TRT data, Walter Brioschi (*Thermogeos srl*) and Roberto Previati (*Soildata srl*) for their fruitful insights on the interpretation of the TRT.

This work has been developed within the MUSA – Multilayered Urban Sustainability Action – project, funded by the European Union – NextGenerationEU, under the National Recovery and Resilience Plan (NRRP) Mission 4 Component 2 Investment Line 1.5: Strengthening of research structures and creation of R&D "innovation ecosystems", set up of "territorial leaders in R&D".

Supplementary materials

Supplementary material associated with this article can be found, in the online version, at doi:10.1016/j.geothermics.2025.103266.

Data availability

The authors do not have permission to share data.

References

Acuña, J., Mogensen, P., Palm, B., 2011. Distributed thermal response tests on a multi-pipe coaxial borehole heat exchanger. HVAC R Res. 17, 1012–1029. https://doi.org/10.1080/10789669.2011.625304.

Acuña, J., Palm, B., 2013. Distributed thermal response tests on pipe-in-pipe borehole heat exchangers. Appl. Energy 109, 312–320. https://doi.org/10.1016/j.apenergy.2013.01.024.

Albers, A., Steger, H., Zorn, R., Blum, P., 2024. Evaluating an enhanced thermal response test (ETRT) with high groundwater flow. Geothermal Energy 12, 1–22. https://doi.org/10.1186/s40517-023-00278-y.

Angelotti, A., Alberti, L., La Licata, I., Antelmi, M., 2014. Energy performance and thermal impact of a Borehole Heat Exchanger in a sandy aquifer: influence of the groundwater velocity. Energy Convers. Manage. 77, 700–708. https://doi.org/10.1016/j.enconman.2013.10.018.

Angelotti, A., Ly, F., Zille, A., 2018. On the applicability of the moving line source theory to thermal response test under groundwater flow: considerations from real case studies. Geothermal Energy 6. https://doi.org/10.1186/s40517-018-0098-z.

Antelmi, M., Alberti, L., Angelotti, A., Curnis, S., Zille, A., Colombo, L., 2020. Thermal and hydrogeological aquifers characterization by coupling depth-resolved thermal response test with moving line source analysis. Energy Convers. Manage. 225, 113400. https://doi.org/10.1016/j.enconman.2020.113400.

Aresti, L., Christodoulides, P., Florides, G., 2018. A review of the design aspects of ground heat exchangers. Renew. Sustain. Energy Rev. 92, 757–773. https://doi.org/10.1016/j.rser.2018.04.053.

Aresti, L., Florides, G.A., Christodoulides, P., 2016. Computational modelling of a ground heat exchanger with groundwater flow. Bulgarian Chem. Commun. 48, 55–63.

Barla, M., Baralis, M., Insana, A., Zacco, F., Aiassa, S., Antolini, F., Azzarone, F., Marchetti, P., 2019. Feasibility study for the thermal activation of Turin Metro Line 2. Tunnels and Underground Cities. Engineering and Innovation Meet Archaeology, Architecture and Art. CRC Press, pp. 231–240.

Bayer, P., Saner, D., Bolay, S., Rybach, L., Blum, P., 2012. Greenhouse gas emission savings of ground source heat pump systems in Europe: a review. Renew. Sustain. Energy Rev. 16, 1256–1267. https://doi.org/10.1016/j.rser.2011.09.027.

Blum, P., Campillo, G., Kölbel, T., 2011. Techno-economic and spatial analysis of vertical ground source heat pump systems in Germany. Energy 36, 3002–3011. https://doi.org/10.1016/j.energy.2011.02.044.

Cai, S., Li, X., Zhang, M., Fallon, J., Li, K., Cui, T., 2020. An analytical full-scale model to predict thermal response in boreholes with groundwater advection. Appl. Therm. Eng. 168, 114828. https://doi.org/10.1016/j.applthermaleng.2019.114828.

Carslaw, H.S., Jaeger, J.C., 1959. Conduction of Heat in Solids, 2nd ed., 1959. Clarendon Press, Oxford.

Chiasson, A.D., Rees, S.J., Spitler, J.D., 2000. A Preliminary Assessment of the Effects of Groundwater Flow On Closed-Loop Ground Source Heat Pump Systems. Oklahoma State Univ, Stillwater, OKUS.

Chiasson, A., O'Connell, A., 2011. New analytical solution for sizing vertical borehole ground heat exchangers in environments with significant groundwater flow: parameter estimation from thermal response test data. HVAC R Res. 17, 1000–1011. https://doi.org/10.1080/10789669.2011.609926.

Claesson, J., Eskilson, P., 1988. Conductive heat extraction to a deep borehole: thermal analyses and dimensioning rules. Energy 13, 509–527.

Curtis, R., Lund, J., Sanner, B., Rybach, L., Hellström, G., 2005. Ground source heat pumps - Geothermal energy for anyone, anywhere: current worldwide activity. Proceed. World Geothermal Cong. 2005, 9.

Dalla Santa, G., Galgaro, A., Sassi, R., Cultrera, M., Scotton, P., Mueller, J., Bertermann, D., Mendrinos, D., Pasquali, R., Perego, R., Pera, S., Di Sipio, E., Cassiani, G., De Carli, M., Bernardi, A., 2020. An updated ground thermal properties database for GSHP applications. Geothermics 85, 101758. https://doi.org/10.1016/j.geothermics.2019.101758.

Dalla Santa, G., Pasquier, P., Schenato, L., Galgaro, A., 2022. Repeated ETRTs in a complex stratified geological setting: high-resolution thermal conductivity identification by multiple linear regression. J. Geotech. Geoenviron. Eng. 148, 1–15. https://doi.org/10.1061/(asce)gt.1943-5606.0002724.

Diao, N., Li, Q., Fang, Z., 2004. Heat transfer in ground heat exchangers with groundwater advection. Int. J. Thermal Sci. 43, 1203–1211. https://doi.org/10.1016/j.ijthermalsci.2004.04.009.

Eskilson, P., 1987. Thermal Analysis of Heat Extraction Boreholes (PhD Thesis). University of Lund.

Festa, A., Dela Pierre, F., Irace, A., Piana, F., Fioraso, G., Lucchesi, S., Boano, P., Forno, M.G., 2009. Note Illustrative della Carta Geologica D'italia Alla Scala 1: 50.000. Foglio 156 - Torino Est. ISPRA.

Galgaro, A., Dalla Santa, G., Zarrella, A., 2021. First Italian TRT database and significance of the geological setting evaluation in borehole heat exchanger sizing. Geothermics 94, 102098. https://doi.org/10.1016/j.geothermics.2021.102098.

Gehlin, S., 2002. Thermal Response Test - Method Development and Evaluation. Lulea University Of Technology, pp. 1402–1544.

Ingersoll, L.R., Zobel, O.J., Ingersoll, A.C., 1954. Heat conduction with engineering, geological and other applications. Fluid Mechan. Appl. https://doi.org/10.1007/978-3-319-15793-1_9.

Kavanaugh, S.P., Rafferty, K., 2014. Geothermal heating and cooling: design of ground-source heat pump systems (ASHRAE).

Lamarche, L., 2023. Fundamentals of Geothermal Heat Pump systems: Design and Application. Springer Nature.

Lo Russo, S., Boffa, C., Civita, M.V., 2009. Low-enthalpy geothermal energy: an opportunity to meet increasing energy needs and reduce CO2 and atmospheric pollutant emissions in Piemonte. Italy Geothermics 38, 254–262. https://doi.org/10.1016/j.geothermics.2008.07.005.

Lo Russo, S., Taddia, G., Baccino, G., Verda, V., 2011. Different design scenarios related to an open loop groundwater heat pump in a large building: impact on subsurface and primary energy consumption. Energy Build. 43, 347–357. https://doi.org/10.1016/j.enbuild.2010.09.026.

Lund, J.W., Huttrer, G.W., Toth, A.N., 2022. Characteristics and trends in geothermal development and use, 1995 to 2020. Geothermics 105, 102522. https://doi.org/10.1016/j.geothermics.2022.102522.

Molina-Giraldo, N., Blum, P., Zhu, K., Bayer, P., Fang, Z., 2011. A moving finite line source model to simulate borehole heat exchangers with groundwater advection. Int. J. Thermal Sci. 50, 2506–2513. https://doi.org/10.1016/j.ijthermalsci.2011.06.012.

Previati, A., Crosta, G., 2024. On groundwater flow and shallow geothermal potential: a surrogate model for regional scale analyses. Sci. Total Environ. 912, 169046. https://doi.org/10.1016/j.scitotenv.2023.169046.

Rivera, J.A., Blum, P., Bayer, P., 2015. Analytical simulation of groundwater flow and land surface effects on thermal plumes of borehole heat exchangers. Appl. Energy 146, 421–433. https://doi.org/10.1016/j.apenergy.2015.02.035.

Saner, D., Juraske, R., Kübert, M., Blum, P., Hellweg, S., Bayer, P., 2010. Is it only CO 2 that matters? A life cycle perspective on shallow geothermal systems. Renew. Sustain. Energy Rev. 14, 1798–1813. https://doi.org/10.1016/j.rser.2010.04.002.

Sanner, B., 2019. Summary of EGC 2019 country update reports on geothermal energy in europe. In: Proceedings of the European Geothermal Congress, p. 18.

Sanner, B., Mands, E., Sauer, M., Grundmann, E., 2008. Thermal Response Test: a routine method to determine thermal ground properties for GSHP design. In: Proc. IEA HPC, pp. 20–22.

Self, S.J., Reddy, B.V., Rosen, M.A., 2013. Geothermal heat pump systems: status review and comparison with other heating options. Appl. Energy 101, 341–348. https://doi.org/10.1016/j.apenergy.2012.01.048.

Shonder, J.A., Beck, J.V., 1999. Field test of a new method for determining soil formation thermal conductivity and borehole resistance. ASHRAe Trans. 106 (1999).

Signorelli, S., Bassetti, S., Pahud, D., Kohl, T., 2007. Numerical evaluation of thermal response tests. Geothermics 36, 141–166. https://doi.org/10.1016/j.geothermics.2006.10.006.

Simon, N., Bour, O., Lavenant, N., Porel, G., Nauleau, B., Pouladi, B., Longuevergne, L., Crave, A., 2021. Numerical and experimental validation of the applicability of Active-DTS experiments to estimate thermal conductivity and groundwater flux in porous media. Water. Resour. Res. 57. https://doi.org/10.1029/2020WR028078.

Spitler, J.D., Bernier, M., 2016. Vertical borehole ground heat exchanger design methods. Advances in Ground-Source Heat Pump Systems. Elsevier Inc., pp. 29–61. https://doi.org/10.1016/B978-0-08-100311-4.00002-9

Spitler, J.D., Gehlin, S.E.A., 2015. Thermal response testing for ground source heat pump systems - An historical review. Renew. Sustain. Energy Rev. 50, 1125–1137. https://doi.org/10.1016/j.rser.2015.05.061.

Stauffer, F., Bayer, P., Blum, P., Molina-Giraldo, N., Kinzelbach, W., 2013. Thermal use of shallow groundwater, thermal use of shallow groundwater. https://doi.org/10.1201/b16239.

Sutton, M.G., Nutter, D.W., Couvillion, R.J., 2003. A ground resistance for vertical bore heat exchangers with groundwater flow. J. Energy Res. Technol., Trans. ASME 125, 183–189. https://doi.org/10.1115/1.1591203.

VDI 4640/2, 2001. Thermal Use of the Underground (German guidelines) — Ground source heat pump systems.

VDI 4640/5, 2020. Thermal use of the underground (German guidelines) — Thermal response test (TRT).

Wagner, V., Blum, P., Kübert, M., Bayer, P., 2013. Analytical approach to groundwater-influenced thermal response tests of grouted borehole heat exchangers. Geothermics 46, 22–31. https://doi.org/10.1016/j.geothermics.2012.10.005.

Wilke, S., Menberg, K., Steger, H., Blum, P., 2020. Advanced thermal response tests: a review. Renew. Sustain. Energy Rev. 119, 109575. https://doi.org/10.1016/j.rser.2019.109575.

Witte, H.J.L., 2013. Error analysis of thermal response tests. Appl. Energy 109, 302–311. https://doi.org/10.1016/j.apenergy.2012.11.060.

Zhang, B., Gu, K., Bayer, P., Qi, H., Shi, B., Wang, B., Jiang, Y., Zhou, Q., 2023. Estimation of groundwater flow rate by an actively heated fiber optics based thermal response test in a grouted borehole. Water Resour. Res. 59. https://doi.org/10.1029/2022WR032672.

Zhao, Z., Lin, Y.F., Stumpf, A., Wang, X., 2022. Assessing impacts of groundwater on geothermal heat exchangers: a review of methodology and modeling. Renew. Energy 190, 121–147. https://doi.org/10.1016/j.renene.2022.03.089.